Published in final edited form as:
Gut. 2014 August ; 63(8): 1333–1344. doi:10.1136/gutjnl-2013-305962.

Myofibroblastic Cells Function as Progenitors to Regenerate Murine Livers after Partial Hepatectomy

M Swiderska-Syn[1], **WK Syn**[1,2], **G Xie**[1], **L Krüger**[1], **MV Machado**[1], **G Karaca**[1], **GA Michelotti**[1], **SS Choi**[1,3], **RT Premont**[1], and **AM Diehl**[1,*]

[1]Division of Gastroenterology, Department of Medicine, Duke University Medical Center, Durham, NC

[2]Regeneration and Repair, Institute of Hepatology, Foundation for Liver Research, London

[3]Section of Gastroenterology, Durham Veterans Affairs Medical Center, Durham, NC

Abstract

Objective—Smoothened (SMO), a co-receptor of the Hedgehog (Hh) pathway, promotes fibrogenic repair of chronic liver injury. We investigated the roles of SMO+ myofibroblasts (MF) in liver regeneration by conditional deletion of SMO in αSMA+ cells after partial hepatectomy (PH).

Design—αSMA-Cre-ER^{T2}×SMO/flox mice were treated with vehicle (Veh) or tamoxifen (TMX), and sacrificed 24 to 96 hrs post-PH. Regenerating livers were analyzed for proliferation, progenitors, and fibrosis by qRT-PCR and quantitative-IHC. Results were normalized to liver-segments resected at PH. For lineage-tracing studies, αSMA-Cre-ER^{T2}×ROSA-Stop-flox-YFP mice were treated with Veh or TMX; livers were stained for YFP, and hepatocytes isolated 48 and 72 hrs post-PH were analysed for YFP by FACS.

Results—Post-PH, Veh-αSMA-SMO mice increased expression of Hh-genes, transiently accumulated MF, fibrosis, and liver progenitors, and ultimately exhibited proliferation of hepatocytes and cholangiocytes. In contrast, TMX-αSMA-SMO mice showed loss of whole liver SMO expression, repression of Hh-genes, enhanced accumulation of quiescent HSC but reduced accumulation of MF, fibrosis, and progenitors, as well as inhibition of hepatocyte and cholangiocyte proliferation, and reduced recovery of liver weight. In TMX-αSMA-YFP mice, many progenitors, cholangiocytes, and up to 25% of hepatocytes were YFP+ by 48-72 h after PH, indicating that liver epithelial cells were derived from αSMA-YFP+cells.

[*]**Corresponding author:** Anna Mae Diehl, MD, Division of Gastroenterology, Duke University Medical Center, 595 LaSalle Street, Snyderman Building, Suite 1073, Durham, NC 27710, 919-684-4173, diehl004@mc.duke.edu.

Conflict of Interest:
All authors declare no conflict of interest in relation to this study

Author contributions:
M.S. designed and performed experiments, analyzed data, and wrote the manuscript; G.X., L.K., M.V.M, and G.K. performed experiments; W.K.S., G.A.M., S.S.C., and R.T.P. wrote the manuscript; A.M.D. designed experiments, supervised research, analyzed data, and wrote the manuscript.

Conclusion—Hedgehog signaling promotes transition of quiescent hepatic stellate cells to fibrogenic MF, some of which become progenitors that regenerate the liver epithelial compartment after PH. Hence, scarring is a component of successful liver regeneration.

Keywords

Epithelial; fibroblasts; hepatic stellate cells; hedgehog; mesenchymal-epithelial transition

Introduction

Adult liver has unique regenerative capabilities as evidenced by its ability to reconstitute functional liver parenchyma within days of 70% partial hepatectomy (PH). It is widely thought that liver regeneration after PH occurs by replication of mature hepatocytes.[1] This belief has hindered understanding of liver repair during a time of remarkable advances in understanding of stem cell biology, provided mainly by studies of tissues where regeneration potential is rather low. Here we revisit liver regeneration after PH using cell lineage tracing, and reveal that a substantial fraction of new hepatocytes are derived from an underappreciated progenitor cell pool within the liver, the hepatic stellate cell, which transitions to a scar-producing myofibroblast (MF) prior to forming a replacement hepatocyte.

PH, like other types of liver injury, triggers MF accumulation and scarring.[2, 3] There is growing evidence that these latter processes occur, at least in part, because liver injury reactivates Hedgehog (Hh) signaling, a fetal morphogenic pathway that is relatively silent in healthy adult livers.[4] Recently, we reported that a population of Hh-responsive cells expressing markers of MF (i.e., alpha smooth muscle actin, αSMA) and hepatic stellate cells (i.e., glial fibrillary acidic protein, GFAP) differentiate into hepatocytes during chronic liver injury.[5] Based on these findings, we postulated that adult hepatic stellate cell (HSC)-derived MF are Hh-regulated, multi-potent progenitors. In the present study, we evaluated the related novel hypothesis that Hedgehog controls liver regeneration after PH by modulating the differentiation of multi-potent myofibroblastic progenitor cells.

Methods

Experimental design

Smo^{tm2Amc}/J (SMO-flox) mice[6] and ROSA-Stop-flox-YFP mice were obtained from The Jackson Laboratory and were crossed with αSMA-Cre-ER^{T2} transgenic mice, which express tamoxifen (TMX)-regulated Cre recombinase under control of the αSMA promoter, as previously described[5]. Double transgenic (DTG) αSMA-Cre × SMO/flox homozygote control mice were bred by crossing SMO/flox homozygote, αSMA-Cre-ER^{T2} hemizygous mice with SMO/flox homozygote mice. Additionally, αSMA-Cre-ER^{T2} × ROSA-Stop-flox-YFP homozygote mice (DTG/YFP) were bred by crossing ROSA-Stop-flox-YFP homozygote, αSMA-Cre-ERT2 hemizygous mice with ROSA-Stop-flox-YFP homozygote mice. Adult (aged 8–12 weeks) mice (n = 167) were subjected to 70% partial hepatectomy[7]. Surgery was performed between 8am and 1230pm for all mice.

In the first experiment, αSMA-Cre-ER^{T2} × SMO/flox DTG mice (n = 55) were divided into groups that received either vehicle or tamoxifen (TMX, 10mg/kg IP, as described below), and then sacrificed at 24 hours (VEH: n = 7; TMX: n= 7), 48 hours (VEH: n = 7;TMX: 7), 72 hours (VEH: n = 6;TMX: n=6), 96 hours (VEH: n = 6; TMX: n= 6) after PH. Smo/flox (single transgenic) STG mice (n = 52) acted as controls in each of the above time point. Because results in all three control groups (i.e., VEH-treated DTG mice, VEH- and TMX-treated STG mice) were similar, data in TMX-treated DTG mice are displayed relative to VEH-treated control DTG mice in the main Results section; results in both groups of STG mice are shown in Supplemental Figure 2.

In the second experiment, αSMA-Cre-ER^{T2} × ROSA-Stop-flox-YFP mice (n = 24) were treated with vehicle or TMX, and then sacrificed at 24 hours (VEH: n = 4; TMX: n = 3), 48 hours (VEH: n = 4; TMX: n = 4), and 72 hours (VEH: n = 4; TMX: n = 4) after PH. *For both first and second experiments*, animals were weighed before PH and at the time of sacrifice; blood and liver samples were obtained. Resected quiescent liver (used as 0-hour comparisons) and regenerating liver remnants were weighed and then formalin fixed or snap frozen in liquid nitrogen.

In the third experiment, we quantified the proportion of hepatocytes that expressed YFP (ie. the progeny of αSMA-positive cells) after PH. To this end, hepatocytes were isolated for FACS analysis (see below) and qRT-PCR (Suppl. Methods). αSMA-Cre-ER^{T2} × ROSA-Stop-flox-YFP (DTG/YFP) mice (n = 16) were used; hepatocytes were isolated at 48 hours (Veh: n = 5; TMX: n = 5), and 72 hours (Veh: n = 3; TMX: n = 3).

As control, another group of αSMA-Cre-ER^{T2} × ROSA-Stop-flox-YFP (DTG/YFP) mice (n = 6) that received TMX were subjected to sham surgery, and hepatocytes isolated at 48 hours (n = 3), and 72 hours (n = 3). Wild type (WT) mice subjected to sham surgery or PH provided further controls (n = 14): 48 hours (sham = 4; PH = 5); 72 hours (sham = 2; PH = 3).

TMX injection

To initiate Cre-mediated gene rearrangement of floxed alleles, DTG or DTG/YFP mice (approximately 25 g in body weight) were injected intraperitoneally with TMX (Sigma-Aldrich) at 10 mg / kg body weight. TMX was first administered at day −4 prior to surgery, and then on alternate days until the day of sacrifice. An equivalent amount of olive oil alone was injected as vehicle control. Because pilot studies demonstrated that Smo mRNA levels in TMX- and VEH-treated mice were similar until 24 h after PH, all studies compared vehicle and TMX-treated mice from 24–96 h after PH.

Liver Cell Isolation and Adenoviral transduction of Hepatic Stellate Cells (HSCs)

Details of hepatocyte and HSC isolation, as well as adenoviral transduction of HSCs are described in Suppl. Methods.

Liver Immunohistochemistry

Details are provided in Suppl. Methods and in Suppl. Table 2.

Molecular Techniques

Two-step real-time RT-PCR and conventional RT-PCR are described in Suppl. Methods and in Suppl. Table 1.

Hydroxyproline assay and Assessment of hepatic injury

Details are provided in Suppl. Methods.

Statistics

All data were expressed as mean ± SEM. Statistical analysis was performed using Student's *t* test or one-way ANOVA as indicated. All analysis was conducted using Graph-Pad Prism 4 software (GraphPad Software Inc.). Differences with $P \leq 0.05$ were considered to be statistically significant.

Results

Conditional loss of SMO in αSMA+ cells decreases hepatic Hh signaling after PH

We created αSMA-Cre-ER^{T2} × SMO/flox double transgenic (DTG) mice where αSMA promoter activity drives expression of Cre recombinase-estrogen receptor fusion and tamoxifen (TMX) treatment sends Cre recombinase into the nucleus to delete the floxed SMO gene, inhibiting Hh signaling selectively in αSMA-expressing cells and their progeny. We confirmed the absence of detectable transgene rearrangement in vehicle-treated DTG mice, and showed that TMX-treated mice exhibit significant loss of the floxed SMO allele and accumulation of the deleted allele only after liver injury, when αSMA is up-regulated.[5]

To investigate how disrupting canonical Hedgehog signaling in MF influences regenerative responses to PH, we injected DTG mice with vehicle or tamoxifen (TMX) and subjected them to PH. In both groups, the quiescent (i.e., pre-PH) liver exhibited minimal Hh pathway activity. Activation of the Hh pathway occurred after PH in vehicle-DTG mice, and the highest mRNA and protein levels of Shh ligand, SMO, Gli1 and Gli2 were seen 24 to 48 hours post PH. PH promoted nuclear GLI2 staining in hepatocytic, ductular, and stromal cells (Supplemental Figure 1). Disruption of SMO in αSMA-expressing cells inhibited Hh signaling after PH. TMX treatment significantly reduced whole liver expression of Smo mRNA and SMO protein in DTG mice (Supplemental Figure 1A, B). Because SMO transduces canonical Hh signaling, the loss of SMO also blocked nuclear accumulation of GLI2 (Supplemental Figure 1C) and led to the concomitant repression of the Hh-target genes, Gli1 and Gli2, to almost basal levels (Supplemental Figure 1D, E). Because many Hh-responsive cells also produce Shh ligand,[8] reduced numbers of GLI2(+) Hh-responsive cells also reduced hepatic expression Shh ligand in TMX-DTG mice (Supplemental Figure 1F). TMX had no effect on any of these parameters in Smo/flox STG mice (Supplemental Figure 2).

Loss of Hh signaling reduces scarring and impairs liver regeneration after PH

As expected,[2, 3] PH provoked scarring. This transient fibrotic response was significantly attenuated in TMX-treated DTG mice, as evidenced by reduced Sirius Red stained collagen fibrils (Figure 1A, B), collagen 1α1 mRNA (Figure 1C), and liver hydroxyproline content

(Figure 1D). MF are the primary cell type responsible for collagen matrix deposition in liver,[9] and an 8 fold increase in αSMA+ cells occurred by 48 hours after PH in vehicle-DTG mice, which was significantly inhibited in TMX-DTG mice. This was paralleled by reduced hepatic expression of αSMA mRNA (Figure 1E). Because most MF appearing during injury are derived from hepatic stellate cells (HSC), we evaluated the expression of desmin (a marker of HSC), as well as vimentin (a mesenchymal marker) by quantitative immunohistochemistry and qRT-PCR. TMX-treated DTG mice accumulate fewer desmin+ and vimentin+ cells after PH (Figure 1E), and expressed less of these mRNAs in whole liver (Figure 1F).

Quiescent HSC are stimulated to become collagen-producing MF by osteopontin (OPN), a Hh-regulated matrix protein that is produced by HSC.[10] In vehicle-treated DTG mice, OPN expression increased 4–5 fold after PH, but loss of SMO in αSMA+ cells repressed OPN gene and protein expression to nearly basal levels (Supplemental Figure 3A, B). OPN is cleaved by matrix metalloproteinase 9 (MMP 9) to form a product that is more potent,[11] and MMP9 induction is necessary for liver regeneration after PH.[12] MMP9 expression mirrored OPN changes after PH, with peak expression of mRNA and protein at 24–48 hours in vehicle-DTG mice, which was significantly attenuated in TMX-DTG mice. MMP9 protein localized mainly in peri-portal sinusoidal cells, and around damaged liver tissue (Supplemental Figure 3C–E). Thus, scarring is a component of the normal regenerative response to PH, and post-PH scarring requires canonical Hh signaling in αSMA+ cells derived from HSC.

To identify other aspects of liver regeneration impacted by disrupting canonical Hh signaling in αSMA+ cells, we compared recovery of liver mass, hepatocyte and cholangiocyte proliferative activity, and functional liver injury in the two groups of mice. Recovery of liver mass after PH was significantly delayed in TMX-DTG mice compared to vehicle-treated mice, indicating impaired liver regeneration (Figure 2A). Loss of Hh signaling in TMX-DTG mice led to significantly fewer hepatocytes and ductular cells with nuclear staining for Ki67, a marker of proliferation (Figure 2B). TMX-DTG liver had worse histologic damage and persistent ALT elevation, indicative of reduced recovery from injury (Figures 2C–E). This requirement for scar-forming cells for liver epithelial regeneration after PH might reflect αSMA+ cell production of trophic factors for liver epithelial progenitors and their progeny. Indeed, TMX-DTG mice had suppressed induction of IL6 and HGF (Figure 2F), two growth factors key for normal regeneration after PH.[1] Given recent evidence that αSMA+ populations include multi-potent progenitors,[5] it is also conceivable that reducing αSMA+ cells removed an important source for replacement liver epithelial cells after PH.

Liver epithelial cells derive from αSMA+ cells after PH

Because rigorous fate mapping studies are required to define the source of new liver epithelial cells following injury, we crossed αSMA-Cre-ER^{T2} mice with ROSA-Stop-flox-YFP mice to generate the DTG/YFP line in which TMX could be used to mark αSMA-expressing cells and their progeny with YFP.[5] Expression of αSMA was not altered by TMX treatment in DTG/YFP mice (Supplemental Figure 4A), and YFP staining was absent

in DTG/YFP mice that were administered vehicle (Figure 3A). However, YFP+ cells were detected from 24 hours post-PH in DTG/YFP mice that had been treated with TMX. At 24 hours post-PH, YFP+ cells were ductular in appearance and localized in Canal of Hering-like structures within zone 1. At 48 and 72 hours after PH, YFP+ cells were mainly found along sinusoids and within plates of hepatic parenchyma in zones 2 and 3 (Figure 3 A–C). Many of these YFP+ cells appeared hepatocytic or ductular and co-expressed Lgr5+ (Figure 3D), a marker for multi-potent progenitors and their immediate progeny in several tissues, including adult liver.[13, 14]

To confirm that YFP+ progeny of αSMA+ cells were epithelial cells, we isolated hepatocytes from vehicle- or TMX-DTG/YFP mice, or wild type controls, 48 and 72 hours after PH, and analyzed direct fluorescence using FACS. Negligible hepatocyte YFP fluorescence was demonstrated after PH in wild type mice, or in TMX-treated, sham-operated DTG/YFP mice (Supplemental Figure 4B). However, 8% and 24% of hepatocytes from TMX-DTG/YFP mice expressed YFP at 48 and 72 hours after PH, indicating that these were derived from αSMA+ cells (Figure 3E). Furthermore, hepatocytes isolated 48 or 72 hours after PH expressed up to 3-fold more Lgr5 mRNA than hepatocytes from undamaged livers (Figure 3F), supporting the hypothesis that Lgr5+ hepatocytes after PH were recently progenitor-derived. We compared Lgr5 expression in HSC and hepatocytes of healthy wild-type mice. Levels of Lgr5 mRNA were more than 10 times higher in quiescent HSC than in hepatocytes (Supplemental Fig 4C). As HSC became myofibroblastic during culture, mRNA expression of Lgr5 declined so that expression of Lgr5 mRNA was similar to that in regenerating hepatocytes 72 h post-PH. At 48 h after PH (when accumulation of αSMA+ cells peaks (Figure 1), immunohistochemistry revealed that most of the Lgr5+ cells localized along sinusoids and had a stellate shape; scattered Lgr5+ hepatocytic and ductular cells were also noted (Supplemental Fig 4D, E). These findings suggest that αSMA+ MF-HSC are the source of the Lgr5+ hepatocytic cells that progressively accumulate post-PH.

Blocking Hh signaling in αSMA+ cells inhibits liver progenitor cell accumulation after PH

Because HSC-derived MF are Hh-responsive, we asked if Hh signaling in αSMA+ cells regulated the accumulation of liver progenitors after PH, by comparing progenitor responses in vehicle-treated and TMX-treated αSMA-Cre-ER^{T2} × SMO/flox DTG mice. We found that inhibiting Hh pathway activity caused a global down-regulation of the liver progenitor response to PH (Figure 4 A, B). For example, Lgr5+ cells increased over 10 fold around portal tracts by 24 hours after PH, and accumulated in zones 2 and 3 by 72–96 hours in vehicle-DTG mice. Lgr5 marked both hepatocytic and ductular cells. In zones 2 and 3, Lgr5+ sinusoidal cells resembling HSC/MF were also particularly prominent, suggesting that regenerating livers normally accumulate Lgr5+ stromal cells (Figure 4C, white arrows). This concept is supported by sinusoidal accumulation of many zone 2–3 YFP+ cells in DTG/YFP double transgenic after PH (Figure 4D; white arrows). Conditional deletion of SMO abrogated accumulation of all types of Lgr5+ cells, and virtually abolished Lgr5 gene and protein expression (Figures 4A, B).

Because YFP+ cells localized in peri-portal Canal of Hering-like structures at 24 h post-PH in our αSMA-lineage tracing study (Figure 3A, B), and others have shown that Sox9+ bi-

potent liver progenitors arise from peri-portal Canals of Hering,[15] we examined this progenitor marker. In vehicle-DTG mice, Sox9+ ductular cells and hepatocytic cells accumulated in peri-portal areas, and Sox9 mRNA was significantly induced, by 24 hours after PH. Sox9+ cell numbers peaked at 48 hours after PH and then returned towards baseline by 96 h post-PH. TMX-DTG mice exhibited almost complete absence of Sox9 mRNA and protein induction post-PH, demonstrating that canonical Hh signaling in αSMA + cells is necessary for Sox9(+) progenitors to accumulate after PH (Figure 4A, B).

Multi-potent Lgr5+ progenitors and bi-potent Sox9+ progenitors can differentiate into either hepatocytes or cholangiocytes.[13, 14, 16] Consistent with this, conditional loss of SMO also reduced accumulation of cells expressing the hepatocyte precursor marker, αfetoprotein (αFP). In vehicle-DTG mice, αFP mRNA increased >4 fold within the initial 24 h after PH and then gradually returned to baseline by 96 h post-PH. αFP+ cells localized peri-portally (i.e., in zone 1) initially, and spread into other parts of liver lobules (i.e., zones 2 and 3) by 72 and 96 hours. These responses were virtually eliminated in TMX-DTG mice after PH (Figure 4A, B). Conditional deletion of SMO also blocked post-PH accumulation of cells expressing keratin 19 (K19), a marker of ductular progenitors and mature cholangiocytes. In vehicle-DTG mice, K19 mRNA levels increased 10–12 fold during the initial 48 h after PH (Figure 4A, B). TMX-DTG mice exhibited near complete repression of K19, plus other progenitor cell markers (muscle pyruvate kinase (MPK), pleiotrophin, and fibroblast growth factor-induced 14 (Fn14)) (Supplemental Figure 5). Loss of SMO in αSMA-expressing cells led to fewer Lgr5+ multi-potent liver progenitor cells, fewer bi-potent Sox9+ progenitors, and fewer progenitor-derived αFP+ hepatocytic and K19+ ductular cells after PH.

Abrogating Hh signaling in αSMA+ cells disrupts transitions that are necessary for effective liver regeneration

Evidence that liver epithelial progenitors derive from Hh-responsive cells that express αSMA, a marker of MF, demonstrates that recovery after PH involves epithelial-mesenchymal transitions (EMT) and mesenchymal-epithelial transitions (MET) of cells in the remnant liver.[17] To investigate whether liver regeneration after PH involves Hh regulation of EMT/MET, we examined liver E-cadherin (Figure 5). E-cadherin expression is typical of epithelial cells, and down-regulation of E-cadherin is a hallmark of EMT.[18] Strong sinusoidal and peri-cellular E-cadherin staining was demonstrated in the livers of both vehicle- and TMX-DTG mice before PH. In the vehicle-treated group, E-cadherin staining and mRNA levels fell significantly by 24 h after PH and remained below basal levels through 96 h post-PH (Figure 5A, B). Deleting SMO in αSMA+ cells after PH maintained pre-PH E-cadherin mRNA levels and pattern of staining. Morphometry showed that E-cadherin expression in TMX-DTG mice was almost twice as high as in vehicle-DTG mice 48 h post-PH, and significantly greater at all post-PH time points evaluated. Differences in E-cadherin mRNA expression were even more pronounced between the two groups (Figure 5B).

Deleting Smo in αSMA+ cells after PH also up-regulated the quiescent HSC markers PPARγ and GFAP by nearly 7 fold (Figure 5A, B), supporting the concept that canonical Hh signaling is necessary for regenerating livers to accumulate HSC-derived MF. Disrupting

that process after PH not only blocks scar formation, but also prevents regeneration of the hepatic epithelial compartment. Interestingly, Hh-dependent epithelial-mesenchymal transitions exhibited zonal differences after PH. Ablating Hh signaling in αSMA+ cells was sufficient to restore E-cadherin loss in zones 1 and 2 at 48 h post-PH, but not in zone 3 (Figure 5C). Thus, the Hh-responsive population of transitional cells that undergo EMT after PH is initially concentrated peri-portally. Because Lgr5+ (and Sox9+) progenitors localize in the peri-portal Canal of Hering compartment (Figures 3, 4), we determined if deleting Smo directly altered expression of Lgr5 in HSC-derived MF from SMO/floxed mice. As noted in Lgr5-expressing HSC from wild type mice (Supplemental Figure 4C), in HSC from SMO/flox mice, mRNA levels of Lgr5 fell as quiescent HSC became αSMA+ MF during culture. Treating SMO/flox MF-HSC with adenoviral vectors for Cre recombinase suppressed their expression of MF markers and restored expression of Lgr5 (Figure 5D). Thus, liver regeneration after PH requires Hh-mediated EMT in peri-portal HSC with multi-potent progenitor capabilities.

Discussion

Our results demonstrate for the first time that regeneration of adult hepatocytes after PH requires Hedgehog (Hh)-dependent modulation of epithelial-mesenchymal transitions (EMT) in multi-potent progenitors that derive from hepatic stellate cells (HSC). These findings contradict two prevailing dogma: first, that EMT does not normally occur during adult liver repair,[19, 20] and second, that liver regenerates after PH because replicatively-quiescent mature hepatocytes abruptly re-enter the cell cycle and proliferate.[21] Our results in the PH model provide compelling support for the heretofore heretical concept that trans-differentiation of resident HSC is a major driver of regeneration following adult liver injury.

Our conclusions were derived by analyzing expression of multiple markers of different liver cell types at several different time points during the first four days after PH in over 50 double transgenic mice and a comparable number of single transgenic controls. The studies relied on analysis of whole liver RNA and quantitative immunohistochemical localization of the respective proteins, and were complemented by lineage tracing studies that examined both intact liver tissue in another two dozen transgenic mice, and isolated cells from an additional three dozen mice to verify the derivation of repopulating hepatocytic cells. These new findings extend earlier data generated by two other groups who also applied fate mapping to determine the source of hepatocytes in regenerating livers after PH.

Malato et al. injected four EYFP reporter mice with AAV8 vectors bearing Cre recombinase under control of regulatory elements of the transthyreitin gene to mark hepatocytes.[22] One week after vector administration, PH was performed and mice were sacrificed on day 21 post-pH. Florescence microscopy of 20 liver sections from these mice demonstrated some EYFP-negative hepatocytic cells near portal areas. Immunostaining for K19 showed that the EYFP-negative cells were K19 negative, confirming the morphological evidence that they were not ductular cells. Although no quantitative data were provided, and the apparent lack of marker expression in hepatocytic cells was not verified by an independent approach, the results support the concept that some of the hepatocytes in day 21 post-PH livers were derived from non-hepatocytic cells, rather than replicating hepatocytes in the liver remnant.

Data interpretation is confounded, however, by the fact that the efficiency of AAV8-mediated gene transfer in adult mice was not reported, and the approach used to deliver Cre recombinase is not absolutely specific for hepatocytes. These are important considerations because uptake of AAV8 by hepatic macrophages is known to limit the effectiveness of liver-directed gene delivery, [23] and adeno-associated viruses have proven to be effective vectors for gene transfer in other liver cell types, such as HSC. [24–26] Also, certain progenitor cells in healthy adult livers express transthyreitin;[27] and the Brenner lab has reported microarray data showing four to twenty-fold induction of transthyreitin mRNA expression in MF-HSC harvested from mice after CCL4 treatment or BDL-induced liver injury. [28]

More recently, the LeClercq lab crossed osteopontin (OPN) Cre^{ERT} mice with EYFP reporter mice in an attempt to track the fate of cholangiocytes and ductular-type progenitor cells after PH.[29] These investigators gave 8 week old adult mice a single injection of TMX, waited one week to perform PH, and then harvested livers for analysis on day 7 post-PH. Fluorescence micrographs display localization of bright EYFP fluorescence in a couple of K19 immuno-stained large duct-like structures near a portal vein, as well as a couple of much smaller ductular structures that were also portal-associated and deemed to be Canals of Herring. The authors concluded that Hepatocyte nuclear factor (HNF) 4-positive hepatocytic cells in the remainder of the liver lobule were EYFP-negative and thus, not derived from ductular cells. However, comparison of the post-PH micrographs with other panels in the same figure suggest that hepatocytes in the one week post-PH livers were generally more fluorescent than hepatocytes in healthy adult livers or hepatocytes in livers two days after acute CCL4 injection. To definitively resolve the question of whether or not hepatocytes were marked by EYFP after PH would require examination of other post-PH time points and analytical approaches that were not employed in this study, such as immunohistochemical analysis of hepatocyte EYFP in intact livers, flow cytometry to directly quantify fluorescence in hepatocytes isolated from regenerating livers of TMX-treated mice and vehicle-treated controls, or analysis of hepatocyte DNA/RNA for evidence of transgene expression. The reproducibility of the microscopy findings is also difficult to judge because the numbers of mice used were not reported and no quantitative data were shown. Data interpretation is further confounded by the fact that expression of OPN, the gene selected to drive Cre recombinase expression, is not restricted to ductular-type cells. Others have demonstrated that other cell types that accumulate during liver injury, such as HSC-derived MF and NKT cells, express OPN mRNA and protein.[10, 30–33] Thus, in our view, neither of the two previous fate mapping studies is informative regarding the role of HSC in regenerating adult hepatocytes after PH. Nevertheless, both papers have been cited as evidence that HSC are not hepatocyte precursors.

Generalized reluctance to acknowledge HSC as potential liver epithelial progenitors stems from the historical focus on HSC's acquisition of myofibroblast (MF) features, including production/destruction of collagen matrix,[34, 35] plus evidence that HSC-derived MF are major producers of collagen matrix during liver scarring.[36] Cirrhosis, the ultimate outcome of progressive MF accumulation and liver scarring, is typically considered to be the antithesis of healthy hepatic regeneration because functional hepatic mass is reduced in cirrhotic livers. We reasoned that such unbalanced outgrowth of MF and hepatocytes might also result when injury disrupts the normal differentiation of a multi-potent progenitor that

generates both MF and hepatocytes. Several lines of evidence now suggest that HSC are more likely than other types of resident liver cells to be multi-potent progenitors.

A key feature of multi-potent progenitors is their ability to acquire characteristics of different cell lineages. Adult HSC co-express mesodermal markers (e.g., Lhx, Wilms tumor-1), ectodermal markers (e.g., Nestin, Glial fibrillary acidic protein),[37–40] and endoderm-enriched genes (e.g., FoxA2, HNF4α, albumin),[5, 41] plus transcription factors associated with stem/progenitor cells (e.g., Nanog, Oct4).[37, 42–45] Depending on culture conditions, HSC from adult livers can generate bone-like, fat-like, neural-like, cholangiocyte-like, or hepatocyte-like cells,[40, 43, 46] demonstrating inherent plasticity. Pancreatic stellate cells (which closely resemble HSC) repopulated the hepatocyte compartment when transplanted after PH,[47] suggesting that some HSC can be re-programmed *in vivo*. That HSC are particularly permissive to re-programming is supported by fate-mapping studies in three distinct mouse strains and two different models of chronic liver injury, all of which demonstrated that hepatocytes and cholangiocytes can be derived from cells that express HSC-enriched genes.[5, 42] HSC are also the only type of resident adult liver cell for which there is unambiguous *in situ* evidence for epithelial-mesenchymal transitions.[5] Such transitions are now acknowledged to be an essential component of stem/progenitor cell reprogramming during development, carcinogenesis, and the generation of induced pluripotent stem cells.[48, 49] The present evidence that PH, the classical model for effective liver regeneration, must first trigger HSC EMT, accumulation of HSC-derived MF, scarring, and outgrowth of MF-derived progenitors in order to effectively regenerate mature liver epithelial cells and restore lost liver mass provides compelling evidence that adult HSC provide a pool of multi-potent progenitors for adult liver repair.

The concept that HSC are resident multi-potent liver progenitors does not nullify the importance of other liver progenitor populations. Rather, it suggests a model whereby various progenitor pools interact to replenish each other. This may be particularly relevant to the bi-potent adult stem-like cells that reside in the smallest branches of the adult biliary tree, widely accepted as being the ultimate precursors of adult hepatocytes and cholangiocytes.[50–54] Lineage tracing approaches have shown that these biliary tree-associated progenitors express Sox9[15] and Foxl1.[55] Recently, expression of Lgr5, a well-accepted marker of multi-potent progenitors in the intestine,[13, 14] was found to be induced in liver 3–6 days after injection of carbon tetrachloride (CCl_4),[56] during the peak of hepatocyte recovery. Lgr5-LacZ mice revealed emergence of LacZ+ cells around small intrahepatic bile ducts 5–6 days after CCl_4 injection.[56] These cells expressed Sox9, and subsequent lineage tracing in various toxin-induced models of liver injury demonstrated that regenerated hepatocytes and cholangiocytes were derived from the Lgr5+ compartment. Curiously, similar to Foxl1+ progenitors,[55] Lgr5+ progenitors did not give rise to either type of liver epithelial cell in the absence of liver injury.[56] Liver injury is also a pre-requisite for hepatic accumulation of MF. Although the authors of the aforementioned CCl4 study reported that they were unable to visualize markers of mature HSC in the Lgr5+ cells that accumulated 5–6 d after CCl_4 injection, the kinetics of Lgr5 induction suggest that its onset coincided with the typical timing of αSMA+ cell accumulation (3–4 days post-CCl_4 treatment).[57] The present study demonstrates that both quiescent HSC and HSC-derived MF express Lgr5, and

HSC-MF are already known to express Sox9[15] and Foxl1.[58] Further, the results identify a previously-unsuspected, and seemingly essential, role for the Hedgehog pathway in regulating the fate of Lgr5+ liver cells after PH. This finding is consistent with earlier gene profiling evidence that Smoothened expression is enriched in Lgr5+ multi-potent liver progenitors.[56]

In summary, there is growing evidence that progenitors are involved in the regeneration of adult liver after many types of chronic injury. Here, we demonstrate that progenitors are equally important for the liver to regenerate after a massive, acute insult, 70% partial hepatectomy (PH). Our studies reveal that effective liver regeneration unexpectedly follows a period of scarring, and show why scarring is important for liver repair, i.e., scar formation is an aspect of epithelial-to-mesenchymal transitions (EMT) in liver-resident multi-potent progenitors, hepatic stellate cells. EMT enhances HSC susceptibility to re-programming, generating the liver epithelial progenitors that differentiate to replace lost hepatocytes and cholangiocytes. Further, we identified a critical role for canonical Hedgehog signaling, an injury-activated morphogenic pathway, in this process. Additional research is needed to determine long term consequences of impairing Hh signaling after acute PH, and to clarify the mechanisms that interface with the Hedgehog pathway to control scarring so that regeneration, rather than cirrhosis, ensues. These discoveries hold the promise of novel diagnostic and therapeutic approaches to improve the outcomes of patients with liver disease.

Supplementary Material

Refer to Web version on PubMed Central for supplementary material.

Acknowledgments

Funding:

This work was supported by the following grants: R37 AA010154 and R01 DK077794 (to A.M. Diehl).

References

1. Michalopoulos GK. Liver regeneration after partial hepatectomy: critical analysis of mechanistic dilemmas. Am J Pathol. 2010; 176:2–13. [PubMed: 20019184]
2. Nakatsukasa H, Evarts RP, Hsia CC, et al. Transforming growth factor-beta 1 and type I procollagen transcripts during regeneration and early fibrosis of rat liver. Lab Invest. 1990; 63:171–180. [PubMed: 2381163]
3. Jakowlew SB, Mead JE, Danielpour D, et al. Transforming growth factor-beta (TGF-beta) isoforms in rat liver regeneration: messenger RNA expression and activation of latent TGF-beta. Cell Regul. 1991; 2:535–548. [PubMed: 1782214]
4. Omenetti A, Choi S, Michelotti G, et al. Hedgehog signaling in the liver. J Hepatol. 2011; 54:366–373. [PubMed: 21093090]
5. Michelotti GA, Xie G, Swiderska M, et al. Smoothened is a master regulator of adult liver repair. J Clin Invest. 2013; 123(6):2380–2394. [PubMed: 23563311]

6. Long F, Zhang XM, Karp S, et al. Genetic manipulation of hedgehog signaling in the endochondral skeleton reveals a direct role in the regulation of chondrocyte proliferation. Development. 2001; 128:5099–5108. [PubMed: 11748145]
7. Ochoa B, Syn WK, Delgado I, et al. Hedgehog signaling is critical for normal liver regeneration after partial hepatectomy in mice. Hepatology. 2010; 51:1712–1723. [PubMed: 20432255]
8. Choi SS, Omenetti A, Syn WK, et al. The role of Hedgehog signaling in fibrogenic liver repair. Int J Biochem Cell Biol. 2011; 43:238–244. [PubMed: 21056686]
9. Kocabayoglu P, Friedman SL. Cellular basis of hepatic fibrosis and its role in inflammation and cancer. Front Biosci (Schol Ed). 2013; 5:217–230. [PubMed: 23277047]
10. Syn WK, Choi SS, Liaskou E, et al. Osteopontin is induced by hedgehog pathway activation and promotes fibrosis progression in nonalcoholic steatohepatitis. Hepatology. 2011; 53:106–115. [PubMed: 20967826]
11. Takafuji V, Forgues M, Unsworth E, et al. An osteopontin fragment is essential for tumor cell invasion in hepatocellular carcinoma. Oncogene. 2007; 26:6361–6371. [PubMed: 17452979]
12. Olle EW, Ren X, McClintock SD, et al. Matrix metalloproteinase-9 is an important factor in hepatic regeneration after partial hepatectomy in mice. Hepatology. 2006; 44:540–549. [PubMed: 16941692]
13. Barker N, Tan S, Clevers H. Lgr proteins in epithelial stem cell biology. Development. 2013; 140:2484–2494. [PubMed: 23715542]
14. Huch M, Boj SF, Clevers H. Lgr5(+) liver stem cells, hepatic organoids and regenerative medicine. Regen Med. 2013; 8:385–387. [PubMed: 23826690]
15. Furuyama K, Kawaguchi Y, Akiyama H, et al. Continuous cell supply from a Sox9-expressing progenitor zone in adult liver, exocrine pancreas and intestine. Nat Genet. 2011; 43:34–41. [PubMed: 21113154]
16. Qiu Q, Hernandez JC, Dean AM, et al. CD24-positive cells from normal adult mouse liver are hepatocyte progenitor cells. Stem Cells Dev. 2011; 20:2177–2188. [PubMed: 21361791]
17. Esteban MA, Bao X, Zhuang Q, et al. The mesenchymal-to-epithelial transition in somatic cell reprogramming. Curr Opin Genet Dev. 2012; 22:423–428. [PubMed: 23084025]
18. Wang Y, Shang Y. Epigenetic control of epithelial-to-mesenchymal transition and cancer metastasis. Exp Cell Res. 2013; 319:160–169. [PubMed: 22935683]
19. Scholten D, Osterreicher CH, Scholten A, et al. Genetic labeling does not detect epithelial-to-mesenchymal transition of cholangiocytes in liver fibrosis in mice. Gastroenterology. 2010; 139:987–998. [PubMed: 20546735]
20. Taura K, Miura K, Iwaisako K, et al. Hepatocytes do not undergo epithelial-mesenchymal transition in liver fibrosis in mice. Hepatology. 2010; 51:1027–1036. [PubMed: 20052656]
21. Michalopoulos GK. Principles of liver regeneration and growth homeostasis. Compr Physiol. 2013; 3:485–513. [PubMed: 23720294]
22. Malato Y, Naqvi S, Schurmann N, et al. Fate tracing of mature hepatocytes in mouse liver homeostasis and regeneration. J Clin Invest. 2011; 121:4850–4860. [PubMed: 22105172]
23. van Dijk R, Montenegro-Miranda PS, Riviere C, et al. Polyinosinic Acid blocks adeno-associated virus macrophage endocytosis in vitro and enhances adeno-associated virus liver-directed gene therapy in vivo. Hum Gene Ther. 2013; 24:807–813. [PubMed: 24010701]
24. Chen M, Wang GJ, Diao Y, et al. Adeno-associated virus mediated interferon-gamma inhibits the progression of hepatic fibrosis in vitro and in vivo. World J Gastroenterol. 2005; 11:4045–4051. [PubMed: 15996030]
25. Suzumura K, Hirano T, Son G, et al. Adeno-associated virus vector-mediated production of hepatocyte growth factor attenuates liver fibrosis in mice. Hepatol Int. 2008; 2:80–88. [PubMed: 19669282]
26. Cong M, Liu T, Wang P, et al. Suppression of tissue inhibitor of metalloproteinase-1 by recombinant adeno-associated viruses carrying siRNAs in hepatic stellate cells. Int J Mol Med. 2009; 24:685–692. [PubMed: 19787203]
27. Sahin MB, Schwartz RE, Buckley SM, et al. Isolation and characterization of a novel population of progenitor cells from unmanipulated rat liver. Liver Transpl. 2008; 14:333–345. [PubMed: 18306374]

28. De Minicis S, Seki E, Uchinami H, et al. Gene expression profiles during hepatic stellate cell activation in culture and in vivo. Gastroenterology. 2007; 132:1937–1946. [PubMed: 17484886]
29. Espanol-Suner R, Carpentier R, Van Hul N, et al. Liver progenitor cells yield functional hepatocytes in response to chronic liver injury in mice. Gastroenterology. 2012; 143:1564–1575. e7. [PubMed: 22922013]
30. Syn WK, Agboola KM, Swiderska M, et al. NKT-associated hedgehog and osteopontin drive fibrogenesis in non-alcoholic fatty liver disease. Gut. 2012; 61:1323–1329. [PubMed: 22427237]
31. Xiao X, Gang Y, Gu Y, et al. Osteopontin contributes to TGF-beta1 mediated hepatic stellate cell activation. Dig Dis Sci. 2012; 57:2883–2891. [PubMed: 22661273]
32. Jiroutova A, Peterova E, Bittnerova L, et al. Collagenolytic potential of rat liver myofibroblasts. Physiol Res. 2013; 62:15–25. [PubMed: 23173684]
33. Coombes J, Syn WK. Utility of osteopontin in lineage tracing experiments. Gastroenterology. 2013; 145:254–255. [PubMed: 23727494]
34. Arthur MJ, Stanley A, Iredale JP, et al. Secretion of 72 kDa type IV collagenase/gelatinase by cultured human lipocytes. Analysis of gene expression, protein synthesis and proteinase activity. Biochem J. 1992; 287(Pt 3):701–707. [PubMed: 1445234]
35. Iredale JP, Goddard S, Murphy G, et al. Tissue inhibitor of metalloproteinase-I and interstitial collagenase expression in autoimmune chronic active hepatitis and activated human hepatic lipocytes. Clin Sci (Lond). 1995; 89:75–81. [PubMed: 7671571]
36. Li D, Friedman SL. Liver fibrogenesis and the role of hepatic stellate cells: new insights and prospects for therapy. J Gastroenterol Hepatol. 1999; 14:618–633. [PubMed: 10440206]
37. Castilho-Fernandes A, de Almeida DC, Fontes AM, et al. Human hepatic stellate cell line (LX-2) exhibits characteristics of bone marrow-derived mesenchymal stem cells. Exp Mol Pathol. 2011; 91:664–672. [PubMed: 21930125]
38. Reister S, Kordes C, Sawitza I, et al. The epigenetic regulation of stem cell factors in hepatic stellate cells. Stem Cells Dev. 2011; 20:1687–1699. [PubMed: 21219128]
39. Kordes C, Sawitza I, Muller-Marbach A, et al. CD133+ hepatic stellate cells are progenitor cells. Biochem Biophys Res Commun. 2007; 352:410–417. [PubMed: 17118341]
40. Kordes C, Sawitza I, Gotze S, et al. Hepatic stellate cells support hematopoiesis and are liver-resident mesenchymal stem cells. Cell Physiol Biochem. 2013; 31:290–304. [PubMed: 23485574]
41. Sicklick JK, Choi SS, Bustamante M, et al. Evidence for epithelial-mesenchymal transitions in adult liver cells. Am J Physiol Gastrointest Liver Physiol. 2006; 291:G575–G583. [PubMed: 16710052]
42. Yang L, Jung Y, Omenetti A, et al. Fate-mapping evidence that hepatic stellate cells are epithelial progenitors in adult mouse livers. Stem Cells. 2008; 26:2104–2113. [PubMed: 18511600]
43. Conigliaro A, Amicone L, Costa V, et al. Evidence for a common progenitor of epithelial and mesenchymal components of the liver. Cell Death Differ. 2013; 20:1116–1123. [PubMed: 23686136]
44. Asahina K. Hepatic stellate cell progenitor cells. J Gastroenterol Hepatol. 2012; 27(Suppl 2):80–84. [PubMed: 22320922]
45. Kordes C, Sawitza I, Haussinger D. Hepatic and pancreatic stellate cells in focus. Biol Chem. 2009; 390:1003–1012. [PubMed: 19642878]
46. Yin C, Evason KJ, Asahina K, et al. Hepatic stellate cells in liver development, regeneration, and cancer. J Clin Invest. 2013; 123:1902–1910. [PubMed: 23635788]
47. Kordes C, Sawitza I, Gotze S, et al. Stellate cells from rat pancreas are stem cells and can contribute to liver regeneration. PLoS One. 2012; 7:e51878. [PubMed: 23272184]
48. Li R, Liang J, Ni S, et al. A mesenchymal-to-epithelial transition initiates and is required for the nuclear reprogramming of mouse fibroblasts. Cell Stem Cell. 2010; 7:51–63. [PubMed: 20621050]
49. Liu X, Sun H, Qi J, et al. Sequential introduction of reprogramming factors reveals a time-sensitive requirement for individual factors and a sequential EMT-MET mechanism for optimal reprogramming. Nat Cell Biol. 2013; 15:829–838. [PubMed: 23708003]
50. Duncan AW, Dorrell C, Grompe M. Stem cells and liver regeneration. Gastroenterology. 2009; 137:466–481. [PubMed: 19470389]

51. Dorrell C, Grompe M. Liver repair by intra- and extrahepatic progenitors. Stem Cell Rev. 2005; 1:61–64. [PubMed: 17132876]
52. Boulter L, Govaere O, Bird TG, Forbes SJ, et al. Macrophage-derived Wnt opposes Notch signaling to specify hepatic progenitor cell fate in chronic liver disease. Nat Med. 2012; 18:572–579. [PubMed: 22388089]
53. Bird TG, Lu WY, Boulter L, et al. Bone marrow injection stimulates hepatic ductular reactions in the absence of injury via macrophage-mediated TWEAK signaling. Proc Natl Acad Sci U S A. 2013; 110:6542–6547. [PubMed: 23576749]
54. Cardinale V, Wang Y, Carpino G, et al. Multipotent stem/progenitor cells in human biliary tree give rise to hepatocytes, cholangiocytes, and pancreatic islets. Hepatology. 2011; 54:2159–2172. [PubMed: 21809358]
55. Sackett SD, Li Z, Hurtt R, et al. Foxl1 is a marker of bipotential hepatic progenitor cells in mice. Hepatology. 2009; 49:920–929. [PubMed: 19105206]
56. Huch M, Dorrell C, Boj SF, et al. In vitro expansion of single Lgr5+ liver stem cells induced by Wnt-driven regeneration. Nature. 2013; 494:247–250. [PubMed: 23354049]
57. Chen Y, Choi SS, Michelotti GA, et al. Hedgehog controls hepatic stellate cell fate by regulating metabolism. Gastroenterology. 2012; 143:1319–1329. e1–11. [PubMed: 22885334]
58. Yin C, Evason KJ, Maher JJ, et al. The basic helix-loop-helix transcription factor, heart and neural crest derivatives expressed transcript 2, marks hepatic stellate cells in zebrafish: analysis of stellate cell entry into the developing liver. Hepatology. 2012; 56:1958–1970. [PubMed: 22488653]

Summary Box

What is already known about the subject?

1. Reprogramming of somatic cells to induced pluripotent stem cells requires a sequential *epithelial-mesenchymal transition (EMT) – mesenchymal-epithelial transition (MET) mechanism* at the start of the reprogramming process
2. During fetal development and in many adult cancers EMT/MET is regulated by Hedgehog, a morphogenic signalling pathway that orchestrates organogenesis by modulating stem/progenitor cell fate.
3. Adult hepatic stellate cells express several stem/progenitor cell markers, and their trans-differentiation into myofibroblasts during culture involves an EMT-like process that is Hedgehog-dependent.
4. During chronic liver injury, sustained activation of the Hedgehog pathway drives accumulation of progenitors and myofibroblasts to promote fibrogenic repair (i.e., scarring).
5. Partial hepatectomy is the ‘gold standard’ model for normal regeneration of mature liver epithelial cells (hepatocytes, cholangiocytes) in healthy adult livers.
6. After partial hepatectomy, Hedgehog signalling increases transiently and drugs that block this inhibit liver regeneration.

What are the new findings?

1. Hepatic stellate cells rapidly undergo a Hedgehog-dependent EMT-like process to generate myofibroblasts that accumulate transiently after partial hepatectomy.
2. Lineage tracing demonstrates that myofibroblasts give rise to liver epithelial progenitors and their progeny (i.e., hepatocytes and cholangiocytes) repopulate the liver after partial hepatectomy
3. After partial hepatectomy, conditionally abrogating Hedgehog signalling in myofibroblasts decreases scarring (i.e., reduces accumulation of myofibroblasts, and fibrosis) but also blocks liver progenitor accumulation, inhibits regeneration of hepatocytes and cholangiocytes, suppresses repair of liver damage, and reduces recovery of liver mass.

How might it impact on clinical practice in the foreseeable future?

1. Biomarkers that reflect deregulated Hedgehog signalling might differentiate individuals whose livers are struggling to recover from injury from those whose livers are regenerating effectively.
2. Drugs might be used to titrate Hedgehog pathway activity up- or down- as needed to enhance regeneration of injured livers.

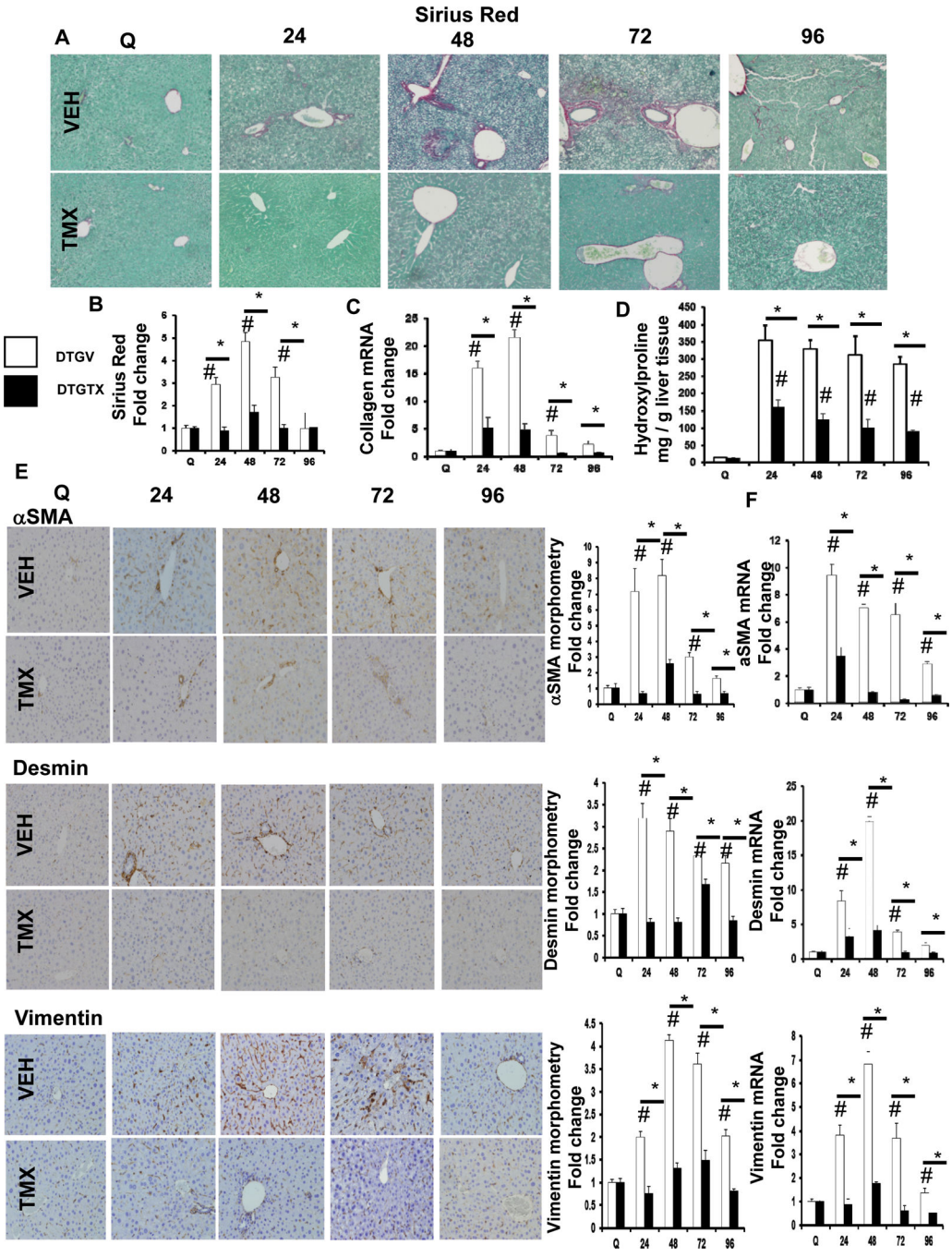

Figure 1. Blocking Hh signaling attenuates fibrogenic outcomes after PH

αSMA-Cre-ER^{T2} × SMO/flox double transgenic (DTG) mice (n = 55) were treated with either vehicle (VEH) or TMX, and then sacrificed at 24 hours (VEH: n=7; TMX: n=7), 48 hours (VEH: n=7; TMX: n=7), 72 hours (VEH: n=6;TMX: n=6), and 96 hours (VEH: n=6; TMX: n=6) after PH. **(A)** Representative liver sections were stained with Sirius Red (SR)/ Fast green to demonstrate collagen fibrils; original magnification x20. **(B)** SR quantification by morphometry; 50 randomly selected, 20x fields were chosen for analysis by the Metaview software **(C)** Total liver RNA was isolated and collagen1α1 mRNA analyzed by

qRT-PCR. **(D)** Quantification of hepatic hydroxyproline in VEH- and TMX-treated groups; data is expressed as mg of hydroxyproline per g of liver tissue. **(E)** Representative liver sections were stained for markers of liver fibrosis, αSMA, Desmin, and Vimentin; original magnification x20. αSMA+, Desmin+, and Vimentin+ cells, respectively, from vehicle- and TMX-treated DTG mice were quantified by morphometry (50 random fields / group; original magnification x20). **(F)** Total liver αSMA, Desmin, and Vimentin mRNA expression. For both morphometric and mRNA data, results are expressed as fold change relative to quiescent liver tissues; mean ± SEM are graphed. Data was analyzed using one-way ANOVA. $^{\#}p<0.05$ compared with quiescent liver; $^{*}p<0.05$ compared with time-matched, Veh-treated group.

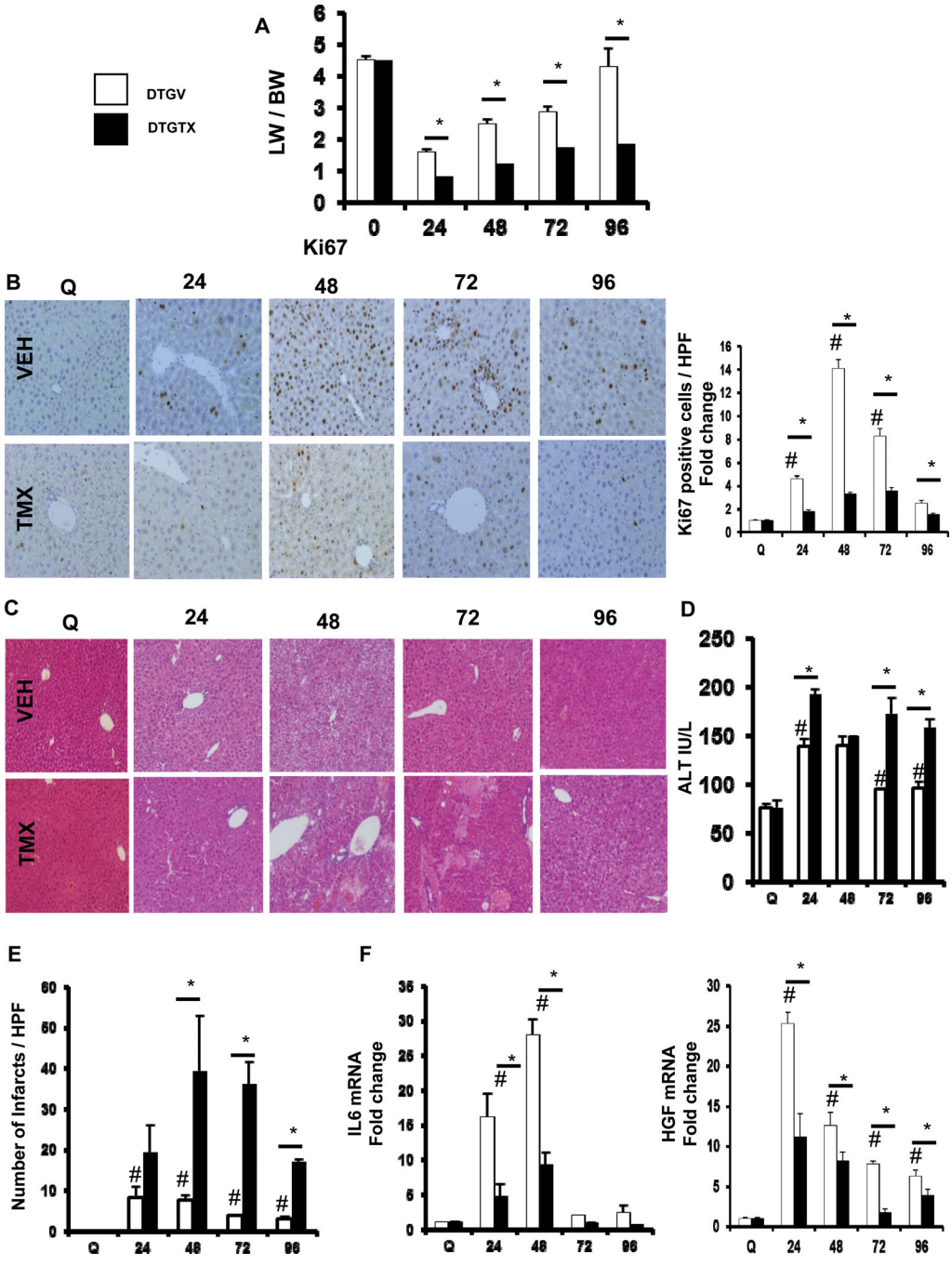

Figure 2. Loss of Hh signaling in αSMA+ cells leads to impaired liver regeneration after PH

DTG mice were treated as described in Figure 1. (A) Liver weight (LW)/Body weight (BW) ratios after PH in VEH- or TMX-treated DTG mice. Results were expressed as fold change relative to quiescent liver tissue. *p<0.05 compared with time-matched VEH-treated mice. **(B)** Representative nuclear Ki67 staining in VEH- and TMX-treated DTG mice. To quantify Ki67+ staining, 20 randomly chosen, 20x fields were evaluated. Results are then expressed as fold change relative to quiescent liver tissues; #p<0.05 compared with quiescent liver; *p<0.05 compared with time-matched, VEH-treated group. **(C)** Representative H&E

staining of liver sections from VEH- and TMX-treated DTG mice. **(D)** Serum levels of alanine aminotransferase (ALT) from both groups of mice; results are graphed as mean ± SEM. **(E)** Number of infarcts per high-powered field (HPF). To quantify infarcts, 50 randomly chosen, 20x fields were evaluated; results graphed as mean ± SEM. **(F)** qRT-PCR analysis of IL6 and HGF expression (two trophic factors) in whole liver mRNA. Results are expressed as fold change relative to quiescent liver tissues; $^{\#}p<0.05$ compared with quiescent liver; $^{*}p<0.05$ compared with time-matched, VEH-treated group.

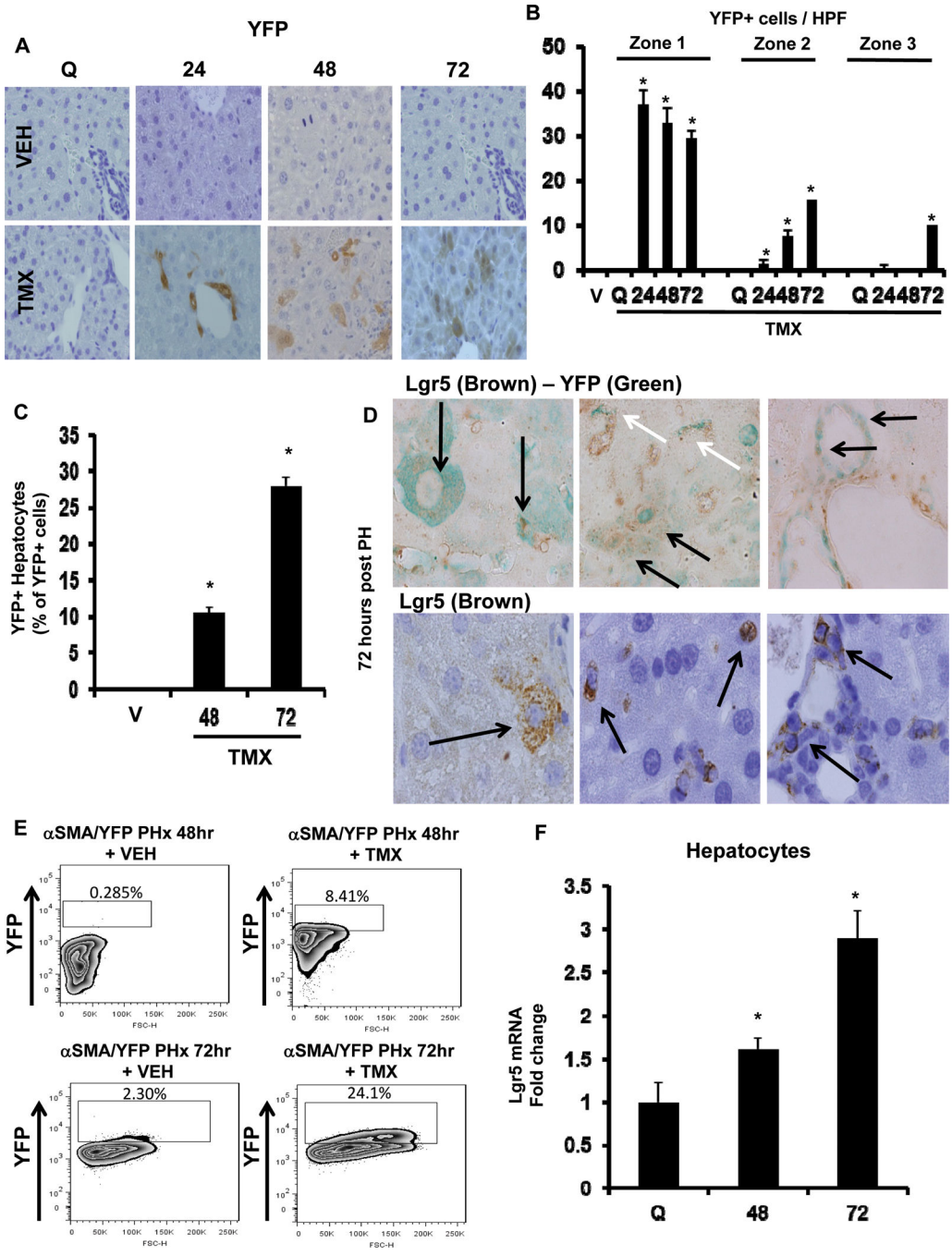

Figure 3. αSMA+ cells are epithelial (hepatocyte and ductular cell) progenitors

αSMA-Cre-ER^{T2} × ROSA-Stop-flox-YFP (DTG/YFP) mice (n=24) were treated with vehicle or TMX, and then sacrificed at 24 hours, 48 hours, and 72 hours after PH. **(A)** Representative immunostaining for hepatic YFP is shown; original magnification x20. **(B)** Zonal quantification of YFP+ cells per HPF; 20 randomly chosen, 20x fields were evaluated. **(C)** Proportion of YFP+ hepatocytes among YFP+ cells per HPF; 40 randomly chosen, 40x fields were evaluated. Results are expressed as mean ± SEM; *p<0.05 compared with VEH-treated group (V). **(D)** Double immunostaining for hepatic Lgr5 (brown) and YFP (green)

(top row) and single immunostaining for hepatic Lgr5 (brown) (bottom row) from TMX-treated DTG/YFP mice are shown. Representative images are shown of hepatocytic, ductular (black arrows), and stromal regions (white arrows). **(E)** Primary hepatocytes were isolated 48 and 72 hours after PH and analyzed for intracellular YFP fluorescence by flow cytometry. The percentages of YFP-positive cells are indicated. **(F)** Primary hepatocytes were isolated 48 and 72 hours after PH in WT mice, and Lgr5 mRNA analyzed by qRT-PCR. Results are expressed as fold change relative to quiescent hepatocytes; mean ± SEM are graphed. *$p<0.05$ compared with quiescent hepatocytes.

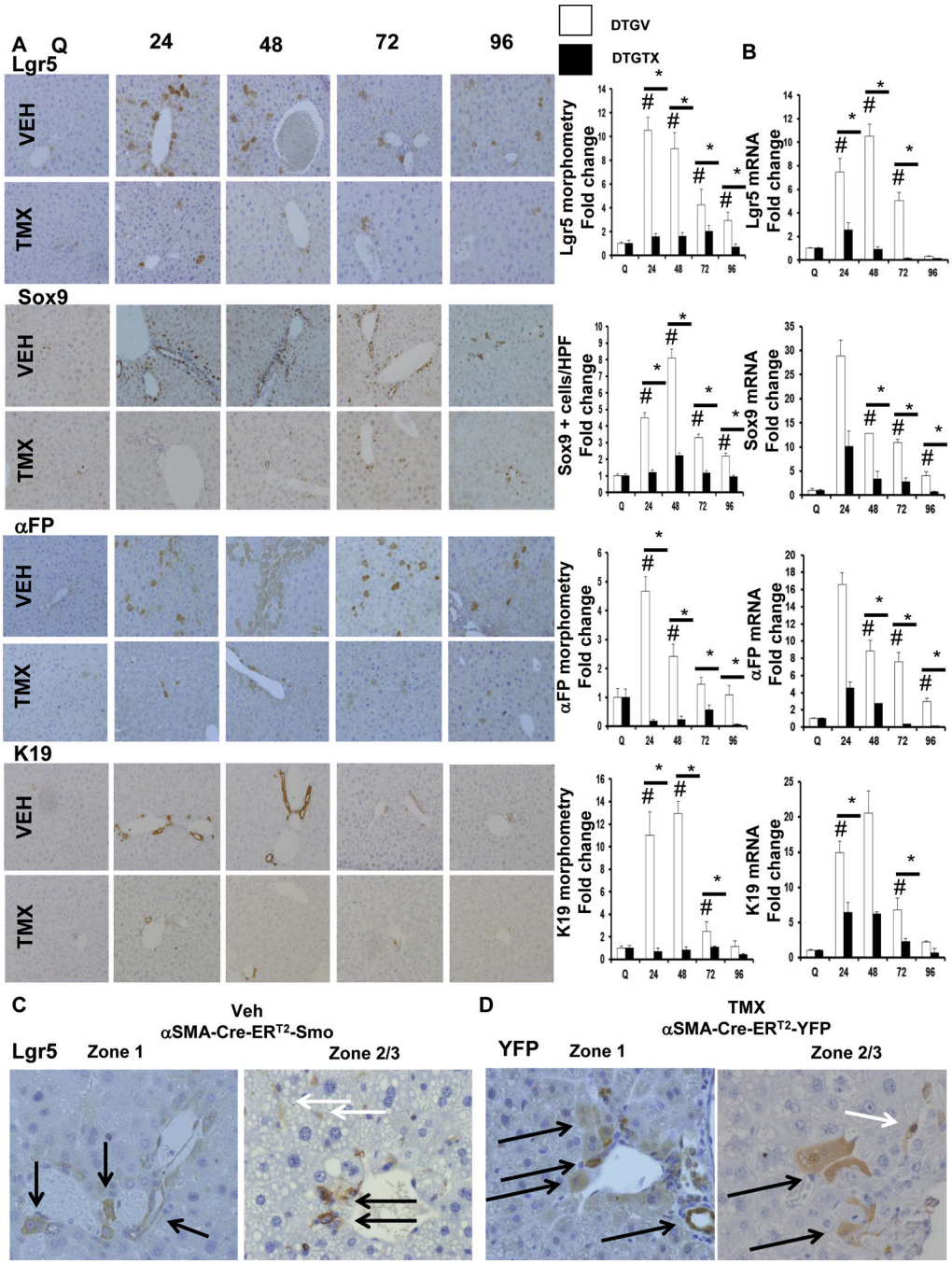

Figure 4. Blocking Hh signaling in αSMA+ cells inhibits liver progenitor cell accumulation after PH

αSMA-Cre-ER^{T2} × SMO/flox DTG mice were treated as described in Figure 1. Representative immunohistochemistry (original magnification x20), morphometric data **(A)** and whole liver mRNA expression **(B)** for Lgr5, Sox9, αFP, and K19. Lgr5+, Sox9+, αFP+, and K19+ cells, respectively, from vehicle- and TMX-treated DTG mice were quantified by morphometry or as number of positive cells per HPF (Lgr5 and αFP: 50 random HPF; Sox9 and K19: 20 random HPF). Results are then expressed as fold change relative to quiescent

liver tissues; mean ± SEM; #p<0.05 compared with quiescent liver; *p<0.05 compared with time-matched, VEH-treated group. **(C)** Zonal pattern of Lgr5 immunoreactivity 72 hours post PH, in VEH-treated DTG mice; black arrows showing Lgr5+ in hepatocytic and ductular cells; white arrows showing Lgr5+ sinusoidal cells resembling HSC/MF. **(D)** Lineage tracing study using DTG/YFP mice (as described in Figure 3) shows corresponding YFP staining in hepatocytic, ductular cells (black arrows), and sinusoidal cells (white arrows) 72 hours post PH.

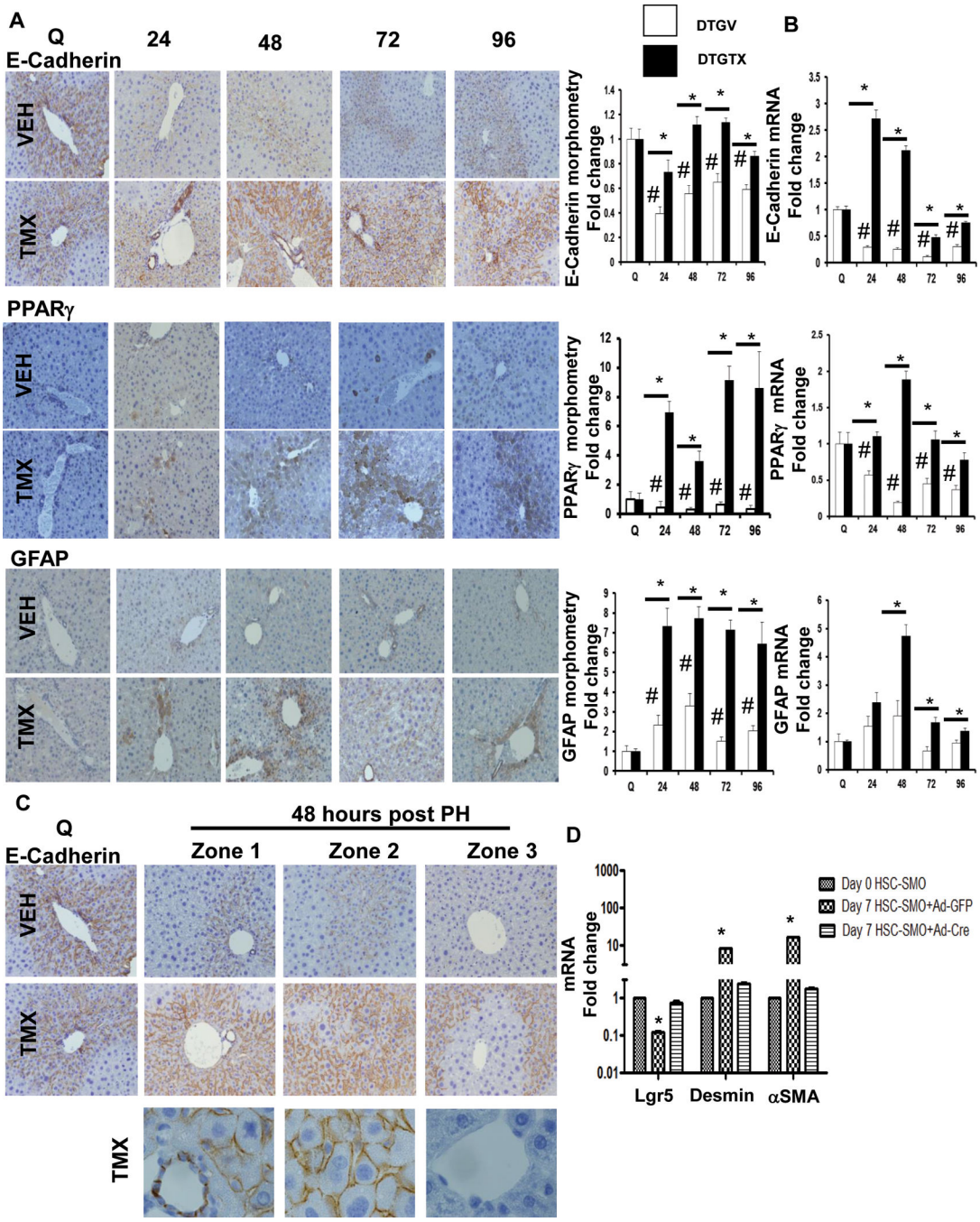

Figure 5. Conditional disruption of SMO in αSMA+ cell disrupts epithelial-mesenchymal transitions and mesenchymal-epithelial transitions necessary for liver regeneration after PH

DTG mice were treated as described in Figure 1. Representative immunohistochemistry, morphometric data **(A)** and whole liver mRNA expression **(B)** for E-Cadherin, PPARγ, and GFAP; original magnification x20. E-Cadherin+, PPARγ+, and GFAP+ cells, respectively, from vehicle- and TMX-treated DTG mice were quantified by morphometry (50 random fields). Results are then expressed as fold change relative to quiescent liver tissues; mean ± SEM; #p<0.05 compared with quiescent liver; *p<0.05 compared with time-matched, VEH-

treated group. **(C)** Zonal pattern of E-cadherin immunostaining at time 0 and 48 hours post PH; bottom panels showing corresponding photomicrographs under high magnification (100x). **(D)** Primary HSC isolated from SMO/flox single transgenic mice were infected with either adenovirus expressing GFP (Ad-GFP, control) or Cre-recombinase (Ad-Cre, for conditional deletion of the Hh signaling intermediate, Smo) on culture day 4. Cells were harvested on culture day 7; lgr5, desmin, and αSMA mRNA analyzed by qRT-PCR. Results are expressed as fold change relative to respective gene expression in day 0 (quiescent) HSC; mean ± SEM; *$p<0.05$ compared with day 0 HSC.